

Application of the Baade-Wesselink method to a pulsating cluster Herbig Ae star: H254 in IC348*

V. Ripepi¹†, R. Molinaro¹, M. Marconi¹, G. Catanzaro², R. Claudi³,
J. Daszyńska-Daszkiewicz⁴, F. Palla⁵, S. Leccia¹, S. Bernabei⁶

¹INAF-Osservatorio Astronomico di Capodimonte, I-80131, Napoli, Italy

²INAF-Osservatorio Astrofisico di Catania, I-95123, Catania, Italy

³INAF-Osservatorio Astronomico di Padova, I-35122, Padova, Italy

⁴Instytut Astronomiczny, Uniwersytet Wrocławski, ul. Kopernika 11, PL-51-622 Wrocław, Poland

⁵INAF-Osservatorio Astrofisico di Arcetri, I-50125, Firenze, Italy

⁶INAF-Osservatorio Astronomico di Bologna, I-40127, Bologna, Italy

ABSTRACT

In this paper we present new photometric and radial velocity data for the PMS δ Sct star H254, member of the young cluster IC 348. Photometric V, R_C, I_C light curves were obtained at the Loiano and Asiago telescopes. The radial velocity data was acquired by means of the SARG@TNG spectrograph. High-resolution spectroscopy allowed us to derive precise stellar parameters and the chemical composition of the star, obtaining: $T_{\text{eff}} = 6750 \pm 150$ K; $\log g = 4.1 \pm 0.4$ dex; $[\text{Fe}/\text{H}] = -0.07 \pm 0.12$ dex. Photometric and spectroscopic data were used to estimate the total absorption in the V band $A_V = 2.06 \pm 0.05$ mag, in agreement with previous estimates. We adopted the technique of the difference in phase and amplitude between different photometric bands and radial velocities to verify that H254 is (definitely) pulsating in a radial mode. This occurrence allowed us to apply the CORS realization of the Baade–Wesselink method to obtain a value for the linear radius of H254 equal to $3.3 \pm 0.7 R_{\odot}$.

This result was used in conjunction with photometry and effective temperature to derive a distance estimate of 273 ± 23 pc for H254, and, in turn for IC 348, the host cluster. This value is in agreement within the errors with the results derived from several past determinations and the evaluation obtained through the Hipparcos parallaxes. Finally, we derived the luminosity of H254 and studied its position in the Hertzsprung–Russell diagram. From this analysis it results that this δ -Scuti occupies a position close to the red edge of the instability strip, pulsates in the fundamental mode, has a mass of about $2.2 M_{\odot}$ and an age of 5 ± 1 Myr, older than previous estimates.

Key words: stars: pre-main-sequence – stars: variables: T Tauri, Herbig Ae/Be – stars: variables: δ Scuti – stars: fundamental parameters – stars: abundances – open clusters and associations: individual: IC 348.

1 INTRODUCTION

Herbig Ae/Be stars (Herbig 1960) are intermediate-mass stars ($1.5 M_{\odot} < M \lesssim 4.5 M_{\odot}$) experiencing their pre-main-

sequence (PMS) phase. Observationally, these stars show: i) spectral type B, A or early F; ii) Balmer emission lines in the stellar spectrum; iii) Infrared radiation excess (in comparison with normal stars) due to circumstellar dust. Additionally, often these objects show significant photometric and spectroscopic variability on very different time-scales. Variable extinction due to circumstellar dust causes variations on timescales of weeks, whereas clumps (protoplanets and planetesimals) in the circumstellar disk or chromospheric activity are responsible for hours to days variability (see e.g. Catala 2003).

* Based on observations made with the Italian Telescopio Nazionale Galileo (TNG) operated on the island of La Palma by the Fundación Galileo Galilei of the INAF (Istituto Nazionale di Astrofisica) at the Spanish Observatorio del Roque de los Muchachos of the Instituto de Astrofísica de Canarias

† Please send offprint requests to ripepi@oacn.inaf.it

It is now well established that intermediate-mass PMS stars during contraction towards the main sequence cross the instability strip for more evolved stars. These young, pulsating intermediate-mass stars are collectively called PMS δ Sct and their variability, similarly to the evolved δ Sct variables, is characterized by short periods (~ 0.5 h \div 5 h) and small amplitudes (from less than a millimag to a few hundredths of magnitude, see, e.g. Kurtz & Marang 1995; Ripepi et al. 2003, 2006; Zwintz 2008; Ripepi et al. 2011, and references therein).

The first theoretical investigation of the PMS δ Sct instability strip based on nonlinear convective hydrodynamical models was carried out by Marconi & Palla (1998). In this seminal paper, these authors calculated the instability strip topology for the first three radial modes and showed that the interior structure of PMS stars crossing the instability strip is significantly different from that of more evolved Main Sequence stars (with the same mass and temperature), even though the envelope structures are similar.

The subsequent theoretical works by several Authors (see e.g. Suran et al. 2001; Marconi et al. 2004; Ruoppo et al. 2007; Di Criscienzo et al. 2008; Guenther & Brown 2004, and references therein) showed that, when a sufficient number of observed frequencies are available for a single object (usually a mixture of radial and non-radial modes), the asteroseismic interpretation of the data allows to estimate with good accuracy the position of these variables in the HR diagram and to get insights into the evolutionary status of the studied objects. From the observational point of view, multi-site campaigns (e.g., Ripepi et al. 2003, 2006; Bernabei et al. 2009) and space observations with MOST and CoRoT (e.g., Zwintz et al. 2009, 2011, for NGC2264) were progressively able to provide improved sets of frequencies to be interpreted at the light of asteroseismic theory. Eventually, the comparison between theory and observations allows to obtain stringent constraints on the stellar parameters and the internal structure of these objects.

On the other hand, the asteroseismic techniques are not suitable for monoperoiodic pulsators, for which it is difficult to discern whether the observed mode is radial or not, making it almost impossible to use stellar pulsation theory to constrain the stellar parameters of the star. As demonstrated by various authors (see e.g. Daszyńska-Daszkiewicz, Dziembowski & Pamyatnykh 2003, 2005, and references therein), this problem can be faced by considering amplitude ratios and phase differences from multi-colour photometry and comparing these with models. This procedure allows to estimate the value of the harmonic degree ℓ . However, for monoperoiodic pulsators, an additional possible test to discriminate between radial and non-radial modes is potentially represented by the so-called Baade-Wesselink test. As well known, the Baade-Wesselink method combines photometric and radial velocity data along the pulsation cycle producing as output an estimate of both the radius and the distance of the investigated pulsating star (see Gautschy 1987, for a review). For radially oscillating stars, the line-of-sight motion (responsible for the radial velocity curve) and the subtended area of the star (responsible for the light curve) are in phase, so that the method gives a reasonable estimate of the stellar radius. This occurrence does not hold in the case of non-radial pulsation. In fact, for a

p -mode with $l = 2$, we would obtain a negative value for the radius, while for $l = 1$ the result would be an unrealistically large radius (Unno et al. 1989).

In this context, among the already known PMS δ Scuti variables, the IC 348 cluster member H 254 (Herbig 1998) is an ideal candidate. Indeed, this pre-main sequence star is fairly bright ($V=10.6$ mag) and it has already been found by Ripepi et al. (2002, Paper I hereinafter) to be a monoperoiodic pulsator with $f = 7.406$ c/d (period ≈ 3.24 h) and a peak to peak V amplitude of ~ 0.02 mag. These results were confirmed by Kızılođlu et al. (2005) on the basis of completely independent photometric observations.

A comparison between observations and the radial analysis based on the models by Marconi & Palla (1998) suggests that H254 could be a $2.6 M_{\odot}$ or a $2.3 M_{\odot}$ pulsating in the first overtone or in the fundamental mode respectively. The application of the Baade-Wesselink method to this pulsator would allow us to test this result. Moreover, such an analysis would also provide an estimate of both the radius and the distance of this star, and in turn, its position in the HR Diagram, as well as an independent estimate of poorly known distance to the parent cluster IC 348, the parent cluster, which is poorly known (see Herbig 1998, for a discussion on this topic).

At variance with the case of RR Lyrae and especially Classical Cepheids, Baade-Wesselink application to δ Sct stars is extremely rare in the literature, and concerned only with High Amplitude δ Sct stars (see e.g. Burki & Meylan 1986). This occurrence is probably due to the limited use of δ Sct as distance indicators for extragalactic objects, as well as to the availability of precise Hipparcos parallaxes for several close objects. In addition, there is an observational difficulty in obtaining high precision radial velocity measurements with the short time exposures needed to avoid light curve smearing for these fast pulsators. Hence in this paper we present the first attempt to apply the BW technique to a low amplitude δ Sct star.

The organization of the paper is as follows: in section 2 we present the photometric and spectroscopic observations; in section 3 we discuss the determination of the stellar parameters and the abundance analysis; section 4 reports on the technique used to discriminate between radial and non-radial pulsation in H254; in section 5 we apply the CORS method to derive the linear radius of our target; section 6 discusses the inferred distance and position in the HR diagram; in section 7 we summarize the main achievements of this paper.

2 OBSERVATIONS AND DATA REDUCTION

The Baade-Wesselink method relies on both photometric and radial velocity (RV) observations. To minimize possible phase shifts between light and RV curves, that could represent a significant source of uncertainty in the application of the method, we aimed at obtaining photometric and spectroscopic observations as simultaneous as possible. This was achieved only partially, as shown in Tab.1, where the log of the observations is shown. Indeed, due to the adverse weather conditions, we were able to gather useful photometric data during only two nights, one of which was luckily very close to the spectroscopic ones so that we are confident that

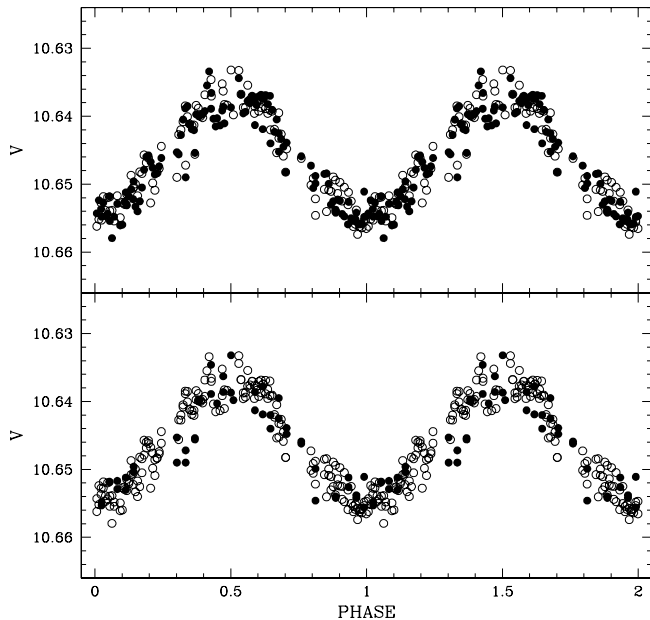


Figure 1. Folded light curve in V for H254. Top panel shows the light curves obtained using H83 (filled circles) and H89 (open circles) as comparison stars, respectively. Bottom panel shows the light curve obtained with the Asiago (filled circles) and Loiano (open circles) telescopes, respectively.

our results are not hampered by the above quoted possible phase shifts.

2.1 Photometry

Photometric data were acquired in the Johnson-Cousins system V , R_C and I_C with the AFOSC¹ and BFOSC² instruments at the 1.8m Asiago and 1.54m Loiano telescopes, respectively. The AFOSC@1.82m instrument was equipped with a TK1024AB 1024x1024 CCD, with a pixel size of $0.47''$ and a total field of view of about $8.1' \times 8.1'$. The BFOSC@1.54m was equipped with a EEV CCD 1300x1340 pixels of individual size $0.58''$, and a total field of view of $13' \times 13'$.

The data were reduced following the usual procedures (de-biasing, flat-fielding) and using standard IRAF³ routines.

To measure the light variations of H254, we adopted the differential photometry technique. We know from Paper I that the stars H83 and H89 are isolated, constant, and bright enough to provide a very high S/N, and hence are the ideal comparison stars.

The aperture photometry was carried out using custom

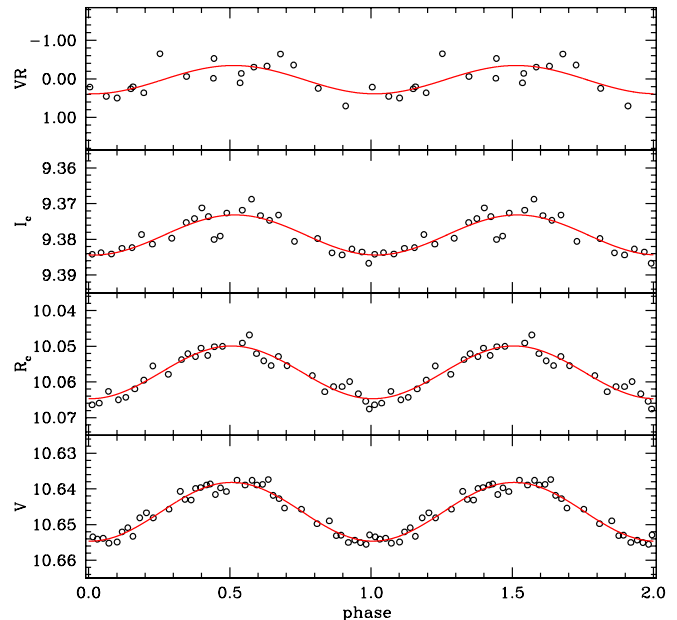


Figure 2. Top panel: folded radial velocity curve of H254. Second to fourth panels show the smoothed folded light curves in I_C , R_C and V , respectively. In all panels the solid line represents a sinusoidal least-squares fit to the data (see text)

routines written in the MIDAS⁴ environment with apertures of about $17''$ for both data sets. To join the Asiago and Loiano observations, we have first calculated the differences in average magnitude between the two sets (of differential magnitudes) due to long term photometric variation not caused by pulsation (see Paper I). The correction was of the order of a few hundredths of magnitudes for all the filters. Due to the largest data set, we retained the Loiano photometry as reference and corrected the Asiago one.

To secure the absolute photometric calibration we have first calibrated the comparison stars H83 and H89, using the $VR_C I_C$ photometry by Trullols & Jordi (1997) and then for each star and filter, we added the magnitude differences with respect to H254. In this way we obtained two distinct calibrated time series for each band, as reported in Tab. 2, which is published in its entirety in the on-line version of the paper. The quality of the data at varying the comparison star or the telescope is shown in Fig 1 in the case of the V band, but similar results are obtained for R_C and I_C . Having verified that all the data we gathered are compatible to each other, the next step was to merge all the data sets (at varying the comparison star and the telescope) for each filter. We then smoothed the resulting light curves by applying a box-car-like smoothing algorithm, making it easier to perform a least-squares fit to the data. The smoothed light curves were then fitted with a Fourier series:

$$mag(\phi) = A_0 + \sum_{i=1}^n A_i \sin(2\pi i\phi + \Phi_i). \quad (1)$$

Typically only one harmonic ($n=1$ in the formula above) is

¹ <http://archive.oapd.inaf.it/asiago/2000/2300/2310.html>

² <http://www.bo.astro.it/loiano/observe.htm>

³ IRAF is distributed by the National Optical Astronomy Observatories, which are operated by the Association of Universities for Research in Astronomy, Inc., under cooperative agreement with the National Science Foundation.

⁴ <http://www.eso.org/sci/software/esomidass/>

Table 1. Log of the observations. Starting from the left, the different columns report: the observing mode; Heliocentric Julian Day (HJD) of start and end observations; the length of the time series; the exposure times (in V , R , I_C , respectively for photometry). Note that HJD=HJD-2454000.

Mode	Obs.	HJD-s d	HJD-e d	Length h	Exptime s
Phot.	Loiano	415.308	415.437	3.1	12,9,8
Phot.	Asiago	434.395	434.547	3.6	10,5,6
Spec.	TNG	431.695	431.759	1.5	1020
Spec.	TNG	432.338	432.747	9.8	1020

Table 2. V , R_C , I_C photometry for H254. From left to right we report: HJD (in days); magnitude; filter; comparison star used. Note that HJD=HJD-2400000.

HJD	Mag	filter	Comparison
54434.39491	10.6400	V	H89
54434.40091	10.6389	V	H89
54434.40693	10.6386	V	H89
54434.41081	10.6387	V	H89
54434.42263	10.6413	V	H89
54434.42652	10.6419	V	H89
54434.43035	10.6440	V	H89
54434.43444	10.6425	V	H89
54434.43831	10.6439	V	H89

Table 2 is published in its entirety only in the electronic edition of the journal. A portion is shown here for guidance regarding its form and content.

sufficient to describe the sinusoidal shape data of the target. The goodness of the photometry is testified by the very low rms of the residuals around the fits: 0.0015 mag, 0.0018 mag and 0.0025 mag for V , R_c and I_c bands, respectively.

The result of all these steps is reported in the last three panels of Fig. 2, where, as in Fig.1, we have phased the photometry using the period given in Paper I, and redetermined the epoch of the minimum light (which was better defined with respect to the maximum) on the Loiano data set.

Table 3. Observation log for spectroscopic data. The B star (HD5394) as well as the target template (the spectrum without the iodine cell) were observed during each night to determine the best instrumental profile modelling.

Star	Nr. spectra	Iodine cell	$T_{exp}[s]$	S/N
HD5394	2	Yes	180	> 200
HD5394	4	No	60	> 200
HD5394	4	No	30	> 200
H254	6	No	1800	40 – 45
H254	22	Yes	1020	19–34

2.2 Spectroscopic observations and radial velocity determination

The spectroscopic observations were carried out with the SARG instrument, which is a high-resolution (from $R = 29000$ to $R = 164000$) cross dispersed echelle spectrograph covering a spectral range from $\lambda = 370$ nm to 1000 nm (see Gratton et al. 2001, for details) mounted at Telescopio Nazionale Galileo (TNG, La Palma, Canarie, Spain)⁵.

Using the yellow grism (spectral range 462 – 792 nm) it is possible to insert in the light path a I_2 -cell and have, in this way, a superimposed (and stable) wavelength reference on the spectrum of the star useful for accurate stellar Doppler shifts measurements. The majority of the spectra in our data sample were acquired in this configuration with a resolution of $R = 164000$ during two observing nights (see table 1). A few spectra of the target were acquired without the I_2 -cell for calibration purposes. The reduction of the spectra (bias subtraction and flat fielding correction) was performed using the common IRAF package facilities. To unveil the radial velocity information hidden in the star spectra, we need to reconstruct the spectra of the star together with the superimposed I_2 spectrum, using the measured instrumental profile, a very high resolution I_2 spectrum and a high resolution and high signal to noise spectrum of the star. To model the instrumental profile, it is necessary to obtain a spectrum for a fast rotating B star acquired with and without the iodine cell. A detailed description of the spectra available is shown in Tab. 3.

Besides, using the high resolution I_2 spectra we obtain the instrumental profile deconvolving it by the B star spectrum. After that the observed spectrum of the star is compared with a modeled spectrum of the star using all obtained elements.

The reconstruction of the spectra and the comparison with the observed one are performed using the AUSTRAL code by Endl et al. (2000). This code takes in account the instrumental profile changes among the spectrum subdividing it in 80-120 pixel chunks. For each of these chunk a radial velocity is measured. Usually the spectrum is subdivided in 400-600 chunks to which correspond a radial velocity measurement. The final radial velocity measure is obtained by the mean and standard deviation of all the results of the chunks. The results of the measurement are reported in Fig. 2 and Tab. 4.

3 SPECTRAL TYPE AND ATMOSPHERIC PARAMETERS

The same spectroscopic data used to build the reference spectrum for radial velocity determination can be used to estimate the intrinsic stellar parameters for the target star.

3.1 Determination of effective temperature

Any attempt devoted to a detailed characterization of the chemical abundance pattern in stellar atmospheres is strictly

⁵ Note that SARG was dismissed at TNG and replaced with the HARPS-N spectrograph.

Table 4. Radial velocities for H254 measured with SARG. Note that HJD=HJD-2400000.

HJD d	RV Km/s	σ_{RV} Km/s
54431.69459	0.246	0.235
54431.70765	0.705	0.327
54431.72033	0.214	0.194
54431.73337	0.495	0.322
54431.74605	0.361	0.495
54432.40098	0.452	0.257
54432.41366	0.205	0.300
54432.42647	-0.652	0.490
54432.43916	-0.061	0.442
54432.45197	-0.015	0.324
54432.46467	0.103	0.412
54432.47749	-0.330	0.354
54432.49018	-0.359	0.395
54432.54718	0.258	0.340
54432.60579	-0.305	0.378
54432.61846	-0.645	0.347
54432.72134	-0.530	0.454
54432.73436	-0.142	0.313

linked with the accuracy of effective temperature and surface gravity determination.

In this study, we derived the effective temperature by using the ionization equilibrium criterion. In practice, we adopted as T_{eff} the value that gives the same iron abundance as computed from a sample spectral lines both neutral and in first ionization stage.

First of all, we selected from the TNG spectrum a sample of iron lines with the principal requirement that they do not show any sensitivity to the gravity (this condition has been checked using spectral synthesis) i.e. synthetic lines computed for a wide range of gravities did not show any appreciable variations. We found six lines belonging to FeI and only two to FeII. The list of these lines with their principal atomic parameters is reported in Tab. 5.

For each line, the equivalent width and the central wavelength have been measured with a Gaussian fit using standard IRAF routines. As the main source of errors in the equivalent width measurements is the uncertain position of the continuum, we applied the formula given in Leone et al. (1995), which takes into account the width of the line and the rms of the continuum. According to the S/N of our spectrum and to the rotational velocity of our target ($v \sin i = 85 \pm 2 \text{ km s}^{-1}$, see next section), we found that the error on the equivalent widths is $\approx 20 \text{ m\AA}$.

Then, once fixed the observed equivalent widths, we computed for each spectral line the theoretical curves in the $\log \text{Fe}/N_{\text{tot}} - T_{\text{eff}}$ plane. Since our target is reported in the literature as a F0 star (SIMBAD database), we explored the range in temperature between 6500 K and 7000 K. Calculations have been performed in two separate steps:

- use of ATLAS9 (Kurucz 1993) to compute the LTE atmospheric models
- use of WIDTH9 (Kurucz & Avrett 1981) to derive abundances from single lines.

The locus in common with all the curves showed in

Table 5. List of iron lines used for temperature determinations, $\log gf$ and relative reference are also reported.

Sp. line	$\log gf$	Reference
FeI $\lambda 5371.489$	-1.644	Ralchenko et al. (2008)
FeI $\lambda 5429.696$	-1.879	Ralchenko et al. (2008)
FeI $\lambda 5466.396$	-0.630	Castelli & Hubrig (2004)
FeI $\lambda 5615.644$	-0.615	Castelli & Hubrig (2004)
FeI $\lambda 5624.542$	-0.900	Castelli & Hubrig (2004)
FeI $\lambda 5658.816$	-0.920	Castelli & Hubrig (2004)
FeII $\lambda 4923.927$	-1.320	Ralchenko et al. (2008)
FeII $\lambda 5018.440$	-1.210	Ralchenko et al. (2008)

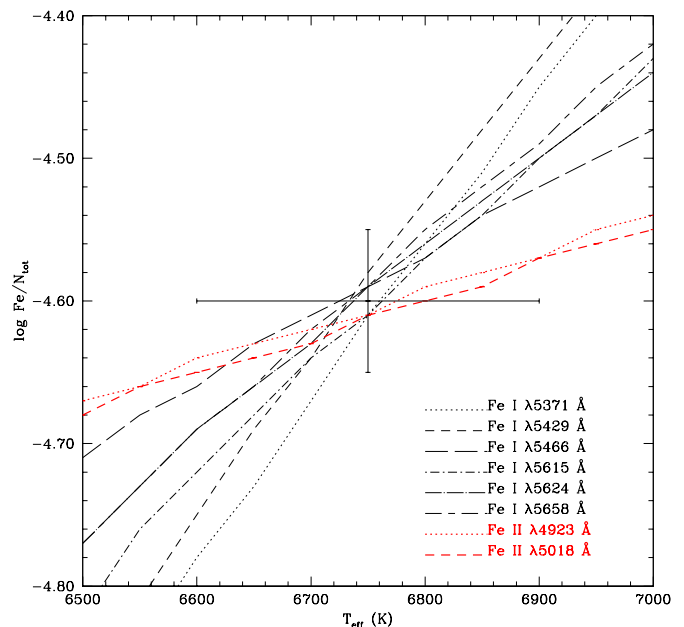

Figure 3. Behaviour of iron abundances as a function of effective temperature. The black curves refer to neutral iron, while the red ones to single ionized.

Fig. 3 represents the effective temperature and iron abundance of H254. To give a realistic estimation of the errors on these values, we repeated the same calculations as before, but varying the EW by a quantity equal to its experimental error. In practice the value of T_{eff} and $\log N_{\text{Fe}}/N_{\text{Tot}}$ derived for $\text{EW} \pm \delta \text{EW}$ gave us the extension of the error bars. Finally, we adopted $T_{\text{eff}} = 6750 \pm 150 \text{ K}$ and $\log N_{\text{Fe}}/N_{\text{Tot}} = -4.60 \pm 0.05$.

3.2 Determination of surface gravity

For early F-type stars, one of the method commonly used in literature for the determination of the luminosity class of stars is to estimate the strength of the ratios between the spectral blend at $\lambda\lambda 4172\text{-}4179 \text{ \AA}$, mostly FeII and TiII lines, and the one at $\lambda 4271 \text{ \AA}$, mostly composed of FeI lines. (Gray & Garrison 1989).

Since the TNG spectra do not cover the spectral region of interest for this purpose, we used the Loiano tele-

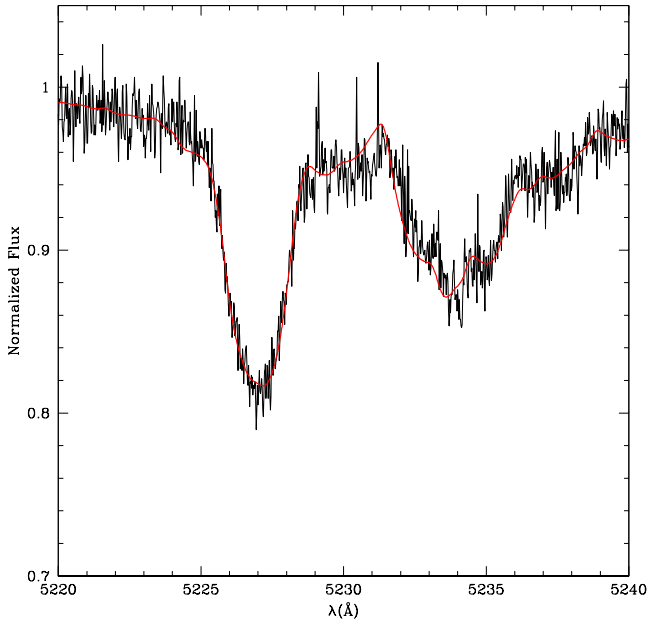


Figure 4. Portion of spectra modeled with $v \sin i = 85 \text{ km s}^{-1}$. The spectral lines are: Fe I $\lambda 5227 \text{ \AA}$ and Fe I $\lambda 5233 \text{ \AA}$.

scope spectra. We computed the $\lambda\lambda 4172\text{-}4179/4271$ ratio which resulted 1.5 ± 0.2 , roughly corresponding to a luminosity class of V (Gray & Garrison 1989).

To go deeply in detail and to derive the surface gravity of our target, we computed the theoretical behaviour of that ratio as a function of $\log g$. After having fixed the T_{eff} to the value found in Sect. 3.1, we computed ATLAS9 atmospheric models with gravities spanning the range between 3.5 and 4.5 dex. By using this curve, we converted our measured ratio in a measurement of gravity, obtaining: $\log g = 4.1 \pm 0.4$.

Finally, considering the results of the Sects. 3.1-3.2, we conclude that the spectral type of our target is F3 V.

3.3 Abundance analysis

To derive chemical abundances, we undertook a synthetic modeling of the observed spectrum. The atmospheric parameters inferred in the previous sections have been adopted to compute an ATLAS9 LTE model with solar ODF. This model has been applied to SYNTH code (Kurucz & Avrett 1981) to compute the synthetic spectrum.

The rotational velocity of H254 has been derived by matching metal lines with synthetic profiles. The best fit occurred for $85 \pm 2 \text{ km s}^{-1}$, where the error has been estimated as the variation in the velocity which increases the χ^2 of a unit. An example of the goodness of our fit is showed in Fig. 4.

Practically, we divided all the spectral range covered by our data in a number of sub-intervals $\approx 100 \text{ \AA}$ wide. For each interval we derived the abundances by a χ^2 minimization of the difference between the observed and synthetic spectrum. Line lists and atomic parameters used in our modeling are from Kurucz & Bell (1995) and the subsequent update

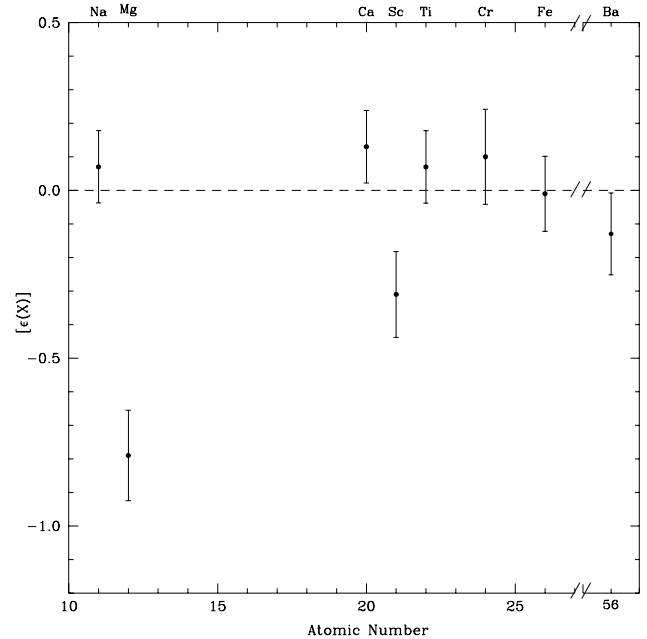


Figure 5. Chemical pattern derived for H254, the horizontal dashed line represents the solar abundances.

by Castelli & Hubrig (2004). The iron abundance found in Sect. 3.1 has been used as guess input to speed up the calculations. The adopted iron abundance with its error is the one reported in Tab. 6.

In Table 6 and Fig. 5 we report the abundances derived in our analysis expressed in the usual logarithmic form relative to the total number of atoms N_{Tot} . To easily compare the chemical pattern of H254 with the Sun, we reported in the last column the differences with the solar values as taken from Asplund et al. (2005). Errors reported in Table 6 for a given element are the standard deviation on the average computed among the various abundances determined in each sub-interval. When a given element appears in one or two sub-intervals only, the error on its abundance evaluated varying temperature and gravity in the ranges $[T_{\text{eff}} \pm \delta T_{\text{eff}}]$ and $[\log g \pm \delta \log g]$ is typically 0.10 dex.

Inspection of Fig. 5 suggests an almost standard atmosphere, with the exception of a moderate under abundance (≈ 0.8 dex) of magnesium and a slight under abundance (≈ 0.3 dex) of scandium.

3.4 Reddening determination

For the following analysis it is important to evaluate the interstellar absorption in the direction of H254. To this aim, we firstly calculated the mean magnitudes in V , R_c and I_c bands on the basis of the fitting curves illustrated in Fig. 2. Then we calculated the colours: $(V - R_c) = 0.589$ mag and $(V - I_c) = 1.268$ mag. Taking advantage of the T_{eff} value estimated from spectroscopy, we can now compare the observed $(V - R_c)$ and $(V - I_c)$ values with those tabulated by Kenyon & Hartmann (1995, their Tab.A5) for the estimated T_{eff} of H254. As a result we find that the tabulated colours are: $(V - R_c) = 0.240$ mag and $(V - I_c) = 0.480$ mag.

Table 6. Chemical abundances derived for the atmosphere of H254. For each element we report its abundance in the form $\log N_{\text{el}}/N_{\text{Tot}}$, and the difference with respect the solar values (Asplund et al. 2005).

Elem.	$\log N_{\text{el}}/N_{\text{Tot}}$	$[\epsilon(x)]$
Na	-5.80 ± 0.10	0.07 ± 0.10
Mg	-5.30 ± 0.10	-0.79 ± 0.13
Ca	-5.60 ± 0.10	0.13 ± 0.11
Sc	-9.30 ± 0.10	-0.31 ± 0.13
Ti	-7.07 ± 0.09	0.07 ± 0.11
Cr	-6.30 ± 0.10	0.10 ± 0.14
Fe	-4.60 ± 0.10	-0.07 ± 0.11
Ba	-10.00 ± 0.10	-0.13 ± 0.12

Hence, the derived values of $E(V - R_c)$ and $E(V - I_c)$ are, respectively, 0.349 mag and 0.788 mag.

The uncertainty on these reddening values has been estimated by analyzing how the theoretical colors change according to the error on the spectroscopic temperature. The resulting uncertainties are $\delta E(V - R_c) = 0.015$ mag and $\delta E(V - I_c) = 0.025$ mag.

From the derived reddening values, we calculated the absorption A_V as the weighted mean of the two values $A_V = 5.956E(V - R_c)$ and $A_V = 2.612E(V - I_c)$, where the numerical coefficients are obtained from Cardelli et al. (1989) assuming $R_V = 3.1$. The value we use in this work is $A_V = 2.06 \pm 0.05$ mag.

4 MODE IDENTIFICATION BY MEANS OF PHASE/AMPLITUDE DIFFERENCE ANALYSIS

Identification of the mode degree, ℓ , for the detected pulsation frequency $\nu = 7.406$ c/d of H254 has been done using the method of Daszyńska-Daszkiewicz, Dziembowski & Pamyatnykh (2003, 2005). In this method the effective temperature perturbation, measured by the complex parameter f , is determined from observation instead of relying on the linear non adiabatic computations of stellar pulsations. The advantage is that we can avoid in that way uncertainties resulting from theoretical modelling, e.g., an impact of subphotospheric convection on pulsation. To apply the quoted method, the VR_{CI} photometric data presented in Sect. 2 are not well suited because of the poor time sampling. Therefore, we adopted the *uvby* Strömgren photometry published in Paper I⁶. In Fig. 6 we show the discriminant χ^2 as a function of ℓ , as determined from the fitting of the theoretical amplitudes and phases to the observational values in all *uvby* passbands, simultaneously. To illustrate how robust is the method to uncertainties in stellar parameters (e.g., effective temperature, luminosity and mass) we considered five models located in the error box of H254.

Moreover, two models of stellar atmospheres were

⁶ We actually published only *b, y* photometry in Paper I. Here we use also the data in the *u, v* bands. The *uvby* light curves are available upon request.

adopted. In the left panel of Fig. 6 we show results obtained with the Kurucz models (Kurucz 2004), whereas the right panel of Fig. 6 reports the same analysis based on the NEMO models (Nendwich et al. 2004). As we can see, in both cases identification of ℓ is clear: the pulsational frequency of H254 is associated with the radial mode.

5 BAADE-WESSELINK APPLICATION TO H254

In section 4 we have show that H254 pulsate in a radial mode. In this section we aim at applying to our target a particular realization of the Baade–Wesselink method called CORS (Caccin et al. 1981) to derive the linear radius, R , of this low amplitude δ -Scuti star. To date, the CORS method has been applied only to Cepheid stars (see Molinaro et al. 2012, and references therein), characterized by light curves with large amplitude (typically ~ 1 mag in the visible) with respect to H254 (~ 0.02 mag). However, considering that: i) the physics governing the pulsation in H254 is the same as in Cepheids and ii) the light curve of H254 seems to be absolutely smooth and not showing any kind of shock (as it happens e.g. for RR Lyrae stars), hence we judge that we can safely apply the CORS method to our target object. This is done in the following section.

5.1 The CORS equation

The basic equation of the CORS method can be easily derived starting from the surface brightness:

$$S_V = m_V + 5 \log \theta \quad (2)$$

where θ is the angular diameter (in mas) of the star and m_V is the apparent magnitude in the V band. If we differentiate eq.(2) with respect to the pulsational phase (ϕ), multiply the result by the generic color index (C_{ij}) and integrate along the pulsational cycle, we obtain:

$$q \int_0^1 \ln \left\{ R_0 - pP \int_{\phi_0}^{\phi} v(\phi') d\phi' \right\} C'_{ij} d\phi - B + \Delta B = 0 \quad (3)$$

where $q = \frac{5}{\ln 10}$, P is the period, v is the radial velocity and p is the projection factor, which correlates radial and pulsational velocities according to $R'(\phi) = -p \cdot P \cdot v(\phi)$. The last two terms, B and ΔB , are given by:

$$B = \int_0^1 C_{ij}(\phi) m'_V(\phi) d\phi \quad (4)$$

$$\Delta B = \int_0^1 C_{ij}(\phi) S'_V(\phi) d\phi. \quad (5)$$

and are connected to the area of the loop described during pulsational cycle of the star, respectively, in the $V-C_{ij}$ plane and S_V-C_{ij} plane, typically with B larger than ΔB .

Equation (3) is an implicit equation in the unknown radius R_0 at an arbitrary phase ϕ_0 . The radius at any phase ϕ can be obtained by integrating the radial velocity curve. The main problem in the solution of eq.(3) is the estimation of the term ΔB which contains the unknown surface brightness. In the case of Cepheids the term ΔB , typically, assumes small values with respect to the B term and, consequently, in the original works it was neglected

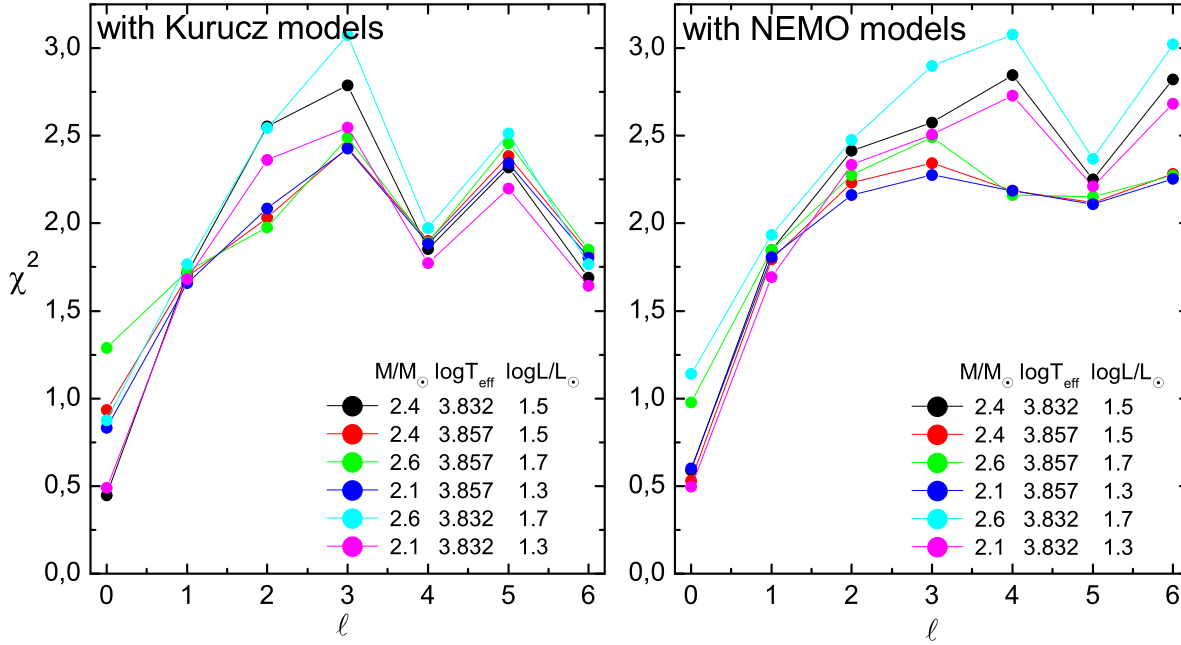


Figure 6. The discriminant, χ^2 as a function of the mode degree, ℓ , for pulsation frequency $\nu = 7.406$ c/d of H254 as obtained from the fit of the photometric amplitudes and phases. The five lines correspond to models consistent with the observations. Two stellar model atmospheres were considered: the Kurucz models (left panel) and The NEMO models (right panel).

(Caccin et al. 1981; Onnembo et al. 1985). However recently Molinaro et al. (2011) found that the Cepheid radii estimated by including the ΔB term are more accurate than those based on the original version of the CORS method.

Ripepi et al. (1997) applied the CORS method to Cepheids and calculated the ΔB term by calibrating the surface brightness expressed as function of the $(V - R_c)$ color index through the relation from Gieren, Barnes & Moffett (1989). In more recent works by Ripepi et al. (2000); Ruoppo et al. (2004) and Molinaro et al. (2011, 2012), the term ΔB has been calculated for a sample of Cepheids by expressing it as a function of two colors using grids of models. In the present work we calibrated the surface brightness using the relations given by Kervella & Fouqué (2008) and taking into account the definition in eq.(2). In particular, we defined the mean surface brightness using the relations in $(V - R_c)$ and $(V - I_c)$ color indices:

$$S_V = \frac{5}{2}(0.5100 + 1.2159(V - R_c) - 0.0736(V - R_c)^2 + 0.4992 + 0.6895(V - I_c) - 0.0657(V - I_c)^2) \quad (6)$$

while the color C_{ij} in the eq.(3) is chosen to be $(V - I_c)$. We note here that the solution of the CORS method is not dependent from the reddening because the first term of the eq.(3) contains the derivative of the color C_{ij} and the two terms B and ΔB are connected with the area of the loops described by the pulsating star.

5.2 The linear radius and the angular diameter

To solve the CORS equation we used the fitted light curves and interpolated the radial velocity data using the same procedure of photometry (see Fig. 2). The rms of residuals of the data around the fitted radial velocity curve is 0.3 km/s. According to our result any phase shift between the minimum of radial velocity and the maximum light is lower than 0.1 times the period, in agreement with other authors (see e.g. Breger et al. 1976; Noskova 1992).

The mean radius obtained from the CORS method is equal to $R = 3.3R_\odot$. To estimate the radius uncertainty we performed Monte Carlo simulations following the same procedure by Caccin et al. (1981). These consist in varying all data points of light and radial velocity curves using random shifts extracted from a Gaussian distribution. The rms of the distribution in the case of photometry is equal to the error on the data points (typically 0.001 mag), while for the radial velocity it is equal to 10% of the amplitude of the radial velocity itself. We have performed 5000 simulations and for each simulated photometry and radial velocity curves the CORS equation has been solved. Finally, the uncertainty has been obtained from the rms of the resulting simulated radius distribution (clipped at 2σ to exclude possible outliers) and is equal to $0.7R_\odot$.

The angular size in mas, θ , of H254 was obtained from the relations provided by Kervella & Fouqué (2008) using $(V - R_c)$ and $(V - I_c)$ colors:

$$\log \theta = 0.5100 + 1.2159(V - R_c) - 0.0736(V - R_c)^2 - 0.2V \quad (7)$$

$$\log \theta = 0.4992 + 0.6895(V - I_c) - 0.0657(V - I_c)^2 - 0.2V \quad (8)$$

with uncertainty of 4.5% and 5.6%, respectively. The derived mean angular diameter is equal to $\theta_1 = 0.120 \pm 0.005$ mas, for the color $(V - R_c)$, and $\theta_2 = 0.088 \pm 0.005$ mas for the color $(V - I_c)$. Hereafter we will use the mean value $0.5(\theta_1 + \theta_2) = 0.104$ mas and, because of the evident inconsistency of the two previous measures, we have conservatively estimated the uncertainty as their half differences $0.5|\theta_1 - \theta_2| = 0.016$ mas. To investigate the dependence of the angular diameter from the reddening, we varied it within the uncertainty reported above and recalculated the angular diameter. The resulting variations (~ 0.001 mas) are included into the error on the mean angular diameter.

6 RESULTS

In this section we derive the distance of H254 and use it to estimate its luminosity. Then, using the spectroscopic effective temperature, we place H254 in the Hertzsprung–Russell diagram to estimate its mass and age using theoretical evolutionary tracks and isochrones from Tognelli et al. (2011).

6.1 The distance of H254

The distance of H254 can be obtained by using the simple equation $d(\text{pc}) = \frac{9.304R(R_\odot)}{\theta(\text{mas})}$, where R is the linear radius derived from the Baade–Wesselink method, θ is the angular diameter, obtained by using the relations by Kervella & Fouqué (2008), and the constant factor takes into account the units of measure. The distance derived in this way is equal to 295 ± 77 pc.

Assuming the validity of the Stefan–Boltzmann law $L = 4\pi R^2 \sigma T_e^2$, where σ is the Stefan–Boltzmann constant and T_e is the effective temperature of the star, the distance can be also calculated from the following equation:

$$d = 10^{0.2(V - A_V + BC_V - M_\odot^{bol} + 10 \log \frac{T}{T_\odot} + 5 \log \frac{R}{R_\odot} + 5)} \quad (9)$$

where BC_V is the bolometric correction from Kenyon & Hartmann (1995), $M_\odot^{bol} = 4.64$ mag is the absolute bolometric magnitude of the Sun (Schmidth–Kaler 1982), $T_\odot = 5777$ K is the Sun effective temperature. The previous equation gives a distance value equal to 262 ± 54 pc. The uncertainty on the previous distance value was obtained from the usual rules of propagation of errors. The value obtained by the solution of the CORS equation is in good agreement with that obtained from the Stefan–Boltzmann law.

A weighted average of the two distance estimates reported above gives 273 ± 23 pc, which represents our best estimate for the distance of the H254.

We tested the consistency of this result with the distance obtained by using the Period–Luminosity relation for δ -Scuti stars. Assuming that H254 pulsate in the fundamental mode (this assumption is justified in the next section), using the PL relation recently derived by McNamara (2011):

$$M_V = (-2.90 \pm 0.05) \log P - (0.19 \pm 0.15)[Fe/H] - (1.27 \pm 0.05)$$

and adopting our metallicity estimate for H254, we obtain an absolute magnitude $M_V = 1.26 \pm 0.07$ mag. By combining

this value with the apparent visual magnitude, $m_V = 10.646$ mag, obtained from the fitting procedure of the data and the extinction $A_V = 2.06$ mag, derived in Sect. 3.4, we obtain a distance equal to 292 ± 15 pc, in very good agreement within the errors with the value from the BW analysis.

In the literature there are other estimates of the distance of H254 and/or the cluster IC 348 harbouring it. Herbig (1998) reviewed all the results till 1998 ranging from low values such as 240_{-84}^{128} pc (Trullols & Jordi 1997) and 260 ± 16 pc (Cernis 1993) to larger values, namely 316 ± 22 pc (Strom, Strom & Carrasco 1974). In the end Herbig (1998) assumed a distance of 316 pc (no error was given).

Subsequent investigations made use of the Hipparcos parallaxes. On the basis of 9 bright members of the cluster, Scholz et al. (1999) derived a distance of 260 ± 25 pc. Contemporaneously, de Zeeuw et al. (1999) estimated the distance of the Per OB2 association, in which IC 348 is supposed to be embedded, and found a value of 318 ± 27 pc. Assuming that there were no mistakes due to the inclusion of non-members to the cluster and/or to the OB association, this discrepancy could mean that the Per OB2 association and IC 348 are not at the same distance. To check this result, we recalculated the distance of IC 348 using the membership criterion by Scholz et al. (1999), but adopting the revised Hipparcos parallaxes by van Leeuwen (2007). The stars selected in this way are listed in Tab. 7 together with the relevant information coming from the satellite. The resulting distance is 227 ± 25 pc, a result which tends to support a lower value for the distance of IC348. This is confirmed even if we include in the calculation only the four stars closer than 30 arcmin to the center of the cluster, obtaining 251 ± 50 pc.

Concluding, our estimate of 273 ± 23 pc is in agreement within the errors with the results derived from the Period–Luminosity relation for δ -Scuti stars by McNamara (2011) and those coming from the Hipparcos parallaxes by Scholz et al. (1999) as well as with the recalculation based on the revised Hipparcos parallaxes by van Leeuwen (2007). We are only marginally in agreement with the larger value of the distance, i.e. 310–320 pc found by Herbig (1998) and de Zeeuw et al. (1999).

6.2 H254 in the Hertzsprung–Russell diagram

Using the distance obtained in the previous section, the apparent magnitude of H254 and our estimate for the absorption, as well as the assumed BC, we can evaluate the intrinsic luminosity of H254. Taking into account the errors associated to the various quantities, we obtain: $\log L/L_\odot = 1.34 \pm 0.08$ dex. The location of the star in the Hertzsprung–Russell diagram (filled red circle in Fig. 7 with the associated error bars), is evaluated combining this luminosity estimate with our spectroscopic measurement of the effective temperature, namely $T_{\text{eff}} = 6750 \pm 150$ K. We notice that the evaluated position of H254 is close to the red edge of the instability strip. In the same plot, the filled blue squares mark the location of the two best fit models, used to define the pulsational mode of H254 (Daszyńska-Daszkiewicz, Dziembowski & Pamyatnykh 2003, 2005). Empirical data seems to suggest that the lower luminosity model with $\log L/L_\odot = 1.3$ should be preferred.

Using the recent results by Tognelli et al. (2011), we overplot in Fig. 7 the evolutionary tracks for selected masses,

Table 7. Data used to recalculate the Hipparcos distance to IC 348. From left to right the different columns show the identification of the star, the distance from the center of IC348, the RA and DEC, the new parallaxes by van Leeuwen (2007), the proper motions in RA and DEC.

name	d arcmin	RA J2000	DEC J2000	π mas	μ_{RA} mas	μ_{DEC} mas
HIP 17465	0.05	03 44 34.187	+32 09 46.14	6.58 ± 4.09	3.49 ± 10.67	-4.86 ± 14.96
HIP 17448	8.13	03 44 19.132	+32 17 17.69	2.91 ± 0.73	8.18 ± 0.70	-10.43 ± 0.69
HIP 17561	21.57	03 45 39.164	+32 26 24.17	6.04 ± 1.59	10.20 ± 1.78	-4.87 ± 1.64
HIP 17631	27.89	03 46 40.871	+32 17 24.68	4.99 ± 0.62	8.53 ± 0.61	-8.29 ± 0.57
HIP 17845	58.12	03 49 07.301	+32 15 51.37	5.29 ± 0.77	10.23 ± 0.81	-8.82 ± 0.74
HIP 17113	60.67	03 39 55.685	+31 55 33.20	5.14 ± 1.06	4.11 ± 1.14	-4.60 ± 0.92
HIP 17052	69.80	03 39 22.934	+32 33 24.39	4.86 ± 1.22	6.52 ± 1.48	-16.53 ± 1.15
HIP 17966	83.50	03 50 27.513	+31 33 13.00	4.57 ± 0.91	8.22 ± 1.06	-6.72 ± 0.90

ranging from $2.0 M_{\odot}$ to $2.8 M_{\odot}$, and three isochrones at 1, 3 and 10 Myr. From this analysis we can conclude that H254 has a mass of about $2.2 M_{\odot}$ and an age of 5 ± 1 Myr. Comparing these results with those obtained in Paper I, we can conclude that H254 has almost the same mass estimated in our previous work, but it results older in the present analysis. Additionally, we note that the radius estimated from the Tognelli et al. (2011) $2.2 M_{\odot}$ evolutionary track at the temperature of H254 is $3.4 R_{\odot}$, in very good agreement with the CORS result.

The solid and dashed magenta lines in Fig. 7 represent the loci of constant fundamental and first overtone period respectively, predicted by linear nonadiabatic models (see Marconi & Palla 1998, for details), with period equal to the observed one. We notice that, even taking into account the errors on the star luminosity and effective temperature, the fundamental mode is favoured.

7 CONCLUSIONS

In this paper we present new photometric and radial velocity data for the PMS δ Sct star H254, member of the young cluster IC 348. The photometric light curves were secured in the Johnson-Cousins V, R_C, I_C bands using the Loiano and Asiago telescopes. The radial velocity data was acquired by means of the SARG@TNG spectrograph. Some of the high-resolution spectra were specifically acquired with SARG to estimate stellar parameters and the chemical composition of the star, obtaining: $T_{\text{eff}} = 6750 \pm 150$ K; $\log g = 4.1 \pm 0.4$ dex; $[\text{Fe}/\text{H}] = -0.07 \pm 0.12$ dex. We note that the T_{eff} derived here is cooler by more than 400 K with respect to previous literature results based on low-resolution spectroscopy. Photometric and spectroscopic data were used to estimate the total absorption in the V band $A_V = 2.06 \pm 0.05$ mag, a value that is in agreement with previous estimates.

To the aim of estimating the radius of H254 by applying a Baade-Wesselink technique, we have first ascertained that H254 pulsate in a radial mode by adopting the technique of the difference in phase and amplitude between different photometric bands and radial velocities. As a result H254 was confirmed to pulsate in a radial mode.

Using the photometric and spectroscopic data, we have applied the CORS realization of the Baade-Wesselink method in the form developed by Ripepi et al. (1997), ob-

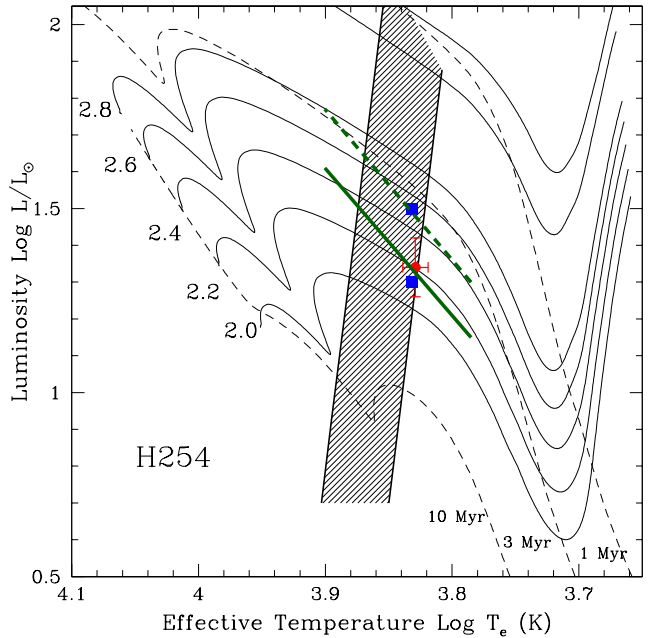


Figure 7. The Hertzsprung–Russell diagram for H254: solid red circle represents the position of H254 obtained by using the spectroscopic temperature and the luminosity derived from the BW analysis. Solid blue squares show the best fit models of Fig. 6. The dark vertical band represents the instability strip from Marconi & Palla (1998), while evolutionary tracks for different values of the mass (solid lines) and the isochrones for different values of the ages (dashed lines) are obtained from Tognelli et al. (2011). Finally, solid and dashed green lines represent the locus of constant period (equal to 7.406^{-1} d) for fundamental and first overtone mode, respectively.

taining a value for the linear radius of H254 equal to $3.3 \pm 0.7 R_{\odot}$. This quantity was used to measure the distance of the target star and, in turn, of the host cluster IC 348, obtaining a final value of 273 ± 23 pc. This estimate is in agreement within the errors with the results derived from the Period–Luminosity relation for δ -Scuti stars by McNamara (2011) and those coming from the Hipparcos parallaxes by Scholz et al. (1999) as well as with our own recalculation based on the revised Hipparcos parallaxes by van Leeuwen

(2007). We are only marginally in agreement with the larger value of the distance, i.e. 310-320 pc found by Herbig (1998) and de Zeeuw et al. (1999).

Finally, we derived the luminosity of H254 and studied its position in the Hertzsprung–Russell diagram. From this analysis it results that this δ -Scuti occupies a position close to the red edge of the instability strip, pulsates in the fundamental mode, has a mass of about $2.2 M_{\odot}$ and an age of 5 ± 1 Myr, older than previous estimates.

ACKNOWLEDGMENTS

We thank our anonymous Referee for his/her very helpful comments that helped in improving the paper. It is a pleasure to thank M.I. Moretti for a critical reading of the manuscript. This research has made use of the SIMBAD database, operated at CDS, Strasbourg, France.

REFERENCES

- Asplund M., Grevesse N., Sauval A. J., 2005, in: “Cosmic Abundances as Records of Stellar Evolution and Nucleosynthesis”, ASP Conference Series, Vol. 336, 25
- Bernabei, S., Riipepi, V., Ruoppo, A., et al. 2009, *A&A*, 501, 279
- Breger, M., Hutchins, J., & Kuhl, L. V. 1976, *ApJ*, 210, 163
- Burki, G., & Meylan, G. 1986, *A&A*, 159, 261
- Caccin, R., Onnembo, A., Russo, G., & Sollazzo, C. 1981, *A&A*, 97, 104
- Cardelli, J. A., Clayton, G. C., & Mathis, J. S. 1989, *ApJ*, 345, 245
- Castelli F., Hubrig S., 2004, *A&A*, 425, 263
- Catala, C. 2003, *Ap&SS*, 284, 53
- Cernis, K. 1993, *Baltic Astronomy*, 2, 214
- Daszyńska-Daszkiewicz J., Dziembowski W.A., Pamyatnykh A.A., 2003, *A&A*, 407, 999
- Daszyńska-Daszkiewicz J., Dziembowski W.A., Pamyatnykh A.A., 2005, *A&A*, 441, 641
- de Zeeuw, P. T., Hoogerwerf, R., de Bruijne, J. H. J., Brown, A. G. A., & Blaauw, A. 1999, *AJ*, 117, 354
- Di Criscienzo, M.; Ventura, P.; D’Antona, F.; Marconi, M.; Ruoppo, A.; Riipepi, V., 2008, *MNRAS*, 389, 325
- Endl, M., Kürster, M., & Els. 2000, *A&A*, 353, L33
- Gautschy, A. 1987, *Vistas in Astronomy*, 30, 197
- Gieren W. P., Barnes, T. G., III, Moffett T. J. 1989, *ApJ*, 342, 467
- Gratton, R., Bonanno, G., Bruno, P. et al. 2001, *Exp. Astron.*, 12, 107
- Gray R. O., Garrison R. F., 1989, *ApJS*, 69, 301
- Guenther, D. B. & Brown, K. I. T. 2004, *ApJ*, 600, 419
- Herbig G. H. 1960, *ApJS*, 4, 337
- Herbig, G. H. 1998, *ApJ*, 497, 736
- Kenyon, S. J., & Hartmann, L. 1995, *ApJS*, 101, 117
- Kervella, P., & Fouqué, P. 2008, *A&A*, 491, 855
- Kızıloğlu, Ü., Kızıloğlu, N., & Baykal, A. 2005, *AJ*, 130, 2766
- Kurtz, D. W., & Marang, F. 1995, *MNRAS*, 276, 191
- Kurucz R. L., Bell B., 1995, Kurucz CD-ROM No. 23. Cambridge, Mass.: Smithsonian Astrophysical Observatory.
- Kurucz R.L., 1993, A new opacity-sampling model atmosphere program for arbitrary abundances. In: Peculiar versus normal phenomena in A-type and related stars, IAU Colloquium 138, M.M. Dworetzky, F. Castelli, R. Faragiana (eds.), A.S.P. Conferences Series Vol. 44, p.87
- Kurucz R.L., Avrett E.H., 1981, *SAO Special Rep.*, 391
- Kurucz R. L. 2004, <http://kurucz.harvard.edu>
- Leone F., Lanzafame A. C., & Pasquini L., 1995, *A&A*, 293, 457
- Marconi, M., & Palla, F. 1998, *ApJ*, 507, L141
- Marconi M., Riipepi V., Palla F., Ruoppo A. 2004, *Comm. in Asteroseismology*, 145, 61
- McNamara, D. H. 2011, *AJ*, 142, 110
- Molinaro, R. et al., 2011, *MNRAS*, 413, 942
- Molinaro, R., Riipepi, V., Marconi, M., et al. 2012, *ApJ*, 748, 69
- Nendwich J., Heiter U., Kupka F., Nesvacil N., Weiss W. W., 2004, *Comm. in Asteroseismology* 144, 43
- Noskova, R. I. 1992, *Soviet Astronomy Letters*, 18, 283
- Onnembo, A., Buonauro, B., Caccin, B., Russo, G., & Sollazzo, C. 1985, *A&A*, 152, 349
- Poretti, E., Clementini, G., Held, E. V., et al. 2008, *ApJ*, 685, 947
- Ralchenko, Yu., Kramida, A.E., Reader, J., and NIST ASD Team (2008). NIST Atomic Spectra Database (version 3.1.5), [Online]. Available: <http://physics.nist.gov/asd3> [2008, December 4]. National Institute of Standards and Technology, Gaithersburg, MD.
- Riipepi, V., Barone, F., Milano, L., & Russo, G. 1997, *A&A*, 318, 797
- Riipepi V., Russo G., Bono G., Marconi M. 2000, *A&A*, 354, 77
- Riipepi, V., Palla, F., Marconi, M., et al. 2002, *A&A*, 391, 587, Paper I
- Riipepi, V., Marconi, M., Bernabei, S., et al. 2003, *A&A*, 408, 1047
- Riipepi, V., Marconi, M., Palla, F. et al. 2006, *Mem. Soc. Astron. It.*, 77, 317
- Riipepi, V., Cusano, F., di Criscienzo, M., et al. 2011, *MNRAS*, 416, 1535
- Ruoppo, A., Riipepi, V., Marconi, M., & Russo, G., 2004, *A&A*, 422, 253
- Ruoppo, V., Marconi, M., Marques, J.P. et al. 2007, *A&A*, 466, 261
- Schmidt–Kaler, T., 1982, in Landolt–Börnstein, Group VI, Vol.2, ed. K.H. Hellwege (Berlin:Springer), 454
- Scholz, R.-D., Brunschendorf, J., Ivanov, G., et al. 1999, *A&AS*, 137, 305
- Strom S. E., Strom K. A., & Carrasco L. 1974, *PASP*, 86, 798
- Suran, M., Goupil, M., Baglin, A., Lebreton, Y., Catala, C. 2001, *A&A*, 372, 233
- Tognelli, E., Prada Moroni, P. G., & Degl’Innocenti, S. 2011, *A&A*, 533, A109
- Trullols E., & Jordi C. 1997, *A&A*, 324, 549
- Unno, W., Osaki, Y., Ando, H., Saio, H., & Shibahashi, H. 1989, *Nonradial oscillations of stars*, Tokyo: University of Tokyo Press, 1989, 2nd ed.,
- van Leeuwen, F. 2007, *A&A*, 474, 653
- Zwintz K. 2008, *ApJ*, 673, 1088
- Zwintz, K., Hareter, M., Kuschnig, R., et al. 2009, *A&A*, 502, 239

Zwintz, K., Kallinger, T., Guenther, D. B., et al. 2011, ApJ,
729, 20